

1
2 **High-efficiency multi-site genomic editing (HEMSE) of *Pseudomonas putida* through**
3 **thermoinducible ssDNA recombineering**

4
5 by

6
7 Tomas Aparicio¹, Akos Nyerges²✉,
8 Esteban Martínez-García*¹ and Víctor de Lorenzo^{1*}

9
10
11 ¹*Systems and Synthetic Biology Program, Centro Nacional de Biotecnología (CNB-CSIC), Campus de*
12 *Cantoblanco, Madrid 28049, Spain* ²*Synthetic and Systems Biology Unit, Institute of Biochemistry,*
13 *Biological Research Centre, Szeged H-6726, Hungary*

14
15
16
17 **Running title:** Multi-site recombineering for *P. putida*

18 **Keywords:** *Pseudomonas*, recombineering, MAGE, DiVERGE, Genome engineering, RBS

19
20
21
22 * Lead Author: Víctor de Lorenzo and Esteban Martínez-García
23 Centro Nacional de Biotecnología-CSIC
24 Campus de Cantoblanco, Madrid 28049, Spain
25 Tel: 34- 91 585 45 36; Fax: 34-91 585 45 06
26 E-mails: vdlorenzo@cnb.csic.es, emartinez@cnb.csic.es
27

28
29 ✉Current address: Harvard Medical School, Boston MA 02115, USA
30

31 SUMMARY

32

33 While single-stranded DNA recombineering is a powerful strategy for higher-scale genome editing, its
34 application to species other than enterobacteria is typically limited by the efficiency of the recombinase
35 and the action of native mismatch repair (MMR) systems. By building on [i] availability of the Erf-like
36 single-stranded DNA-annealing protein Rec2, [ii] adoption of tightly-regulated thermoinducible device
37 and [iii] transient expression of a MMR-suppressing *mutL* allele, we have set up a coherent genetic
38 platform for entering multiple changes in the chromosome of *Pseudomonas putida* with an
39 unprecedented efficacy and reliability. The key genetic construct to this end is a broad host range
40 plasmid encoding co-transcription of *rec2* and *P. putida*'s *mutL*_{E36K}^{PP} at high levels under the control of
41 the *P_L/cI857* system. Cycles of short thermal shifts of *P. putida* cells followed by transformation with a
42 suite of mutagenic oligos delivered different types of high-fidelity genomic changes at frequencies up to
43 10% per single change—that can be handled without selection. The same approach was instrumental to
44 super-diversify short chromosomal portions for creating libraries of functional genomic segments—as
45 shown in this case with ribosomal binding sites. These results enable the multiplexing of genome
46 engineering of *P. putida*, as required for metabolic engineering of this important biotechnological
47 chassis.

48

49

50 INTRODUCTION

51

52 DNA recombineering was first developed in the early 2000s (Datsenko and Wanner, 2000; Yu et al.,
53 2000) as a genetic technology for replacing genomic segments of *E. coli* with synthetic double stranded
54 (ds) DNA by means of the DNA exchange mechanism brought about by the Red system of phage
55 lambda. While the native approach involves 3 proteins (a β -recombinase, an exonuclease and the γ
56 protein which protects free ds-ends of DNA from degradation by RecBCD), it turned out that the Red- β
57 protein sufficed to promote invasion of the replication fork by single-stranded oligonucleotides
58 incorporated as Okazaki fragments (Ellis et al., 2001). If such oligonucleotides were designed to carry
59 mutations, the resulting changes could be inherited at considerable frequencies upon subsequent
60 rounds of DNA segregation. The key value of this approach is that by using cocktails of mutagenic
61 oligonucleotides and either manual or automated cycles of Red expression/oligonucleotide

62 transformation one can enter simultaneous changes in many genomic sites and/or saturate given DNA
63 stretches with specific or random mutations (Wang et al., 2009; Nyerges et al., 2016; Nyerges et al.,
64 2018). These methods have been improved further by using host strains transiently disabled in
65 mismatch repair and by enriching mutants through Cas9/gRNA-based counterselection of wild-type
66 sequences (Costantino and Court, 2003; Jiang et al., 2013; Nyerges et al., 2014; Nyerges et al., 2016;
67 Ronda et al., 2016; Oesterle et al., 2017). While these technologies work well in *E. coli*, they are difficult
68 to transplant directly to non-enteric bacteria. Yet, their applicability to species such as *Pseudomonas*
69 *putida* has a special interest because of the value of environmental microorganisms as useful platforms
70 for metabolic engineering (Nikel et al., 2014; Nikel et al., 2016; Martínez-García and de Lorenzo, 2019).
71 Attempts of functional expression of the lambda Red system in various species of *Pseudomonas* have
72 been reported, but recombination frequencies were low in the absence of selection (Lesic and Rahme,
73 2008; Liang and Liu, 2010; Luo et al., 2016; Chen et al., 2018; Yin et al., 2019). Red-like counterparts
74 found in *Pseudomonas* prophages have been more successful to the same ends. For example, the
75 RecET recombinase/exonuclease pair of *P. syringae* has been instrumental for executing a suite of
76 manipulations in this species (Swingle et al., 2010a; Bao et al., 2012). Furthermore, bioinformatic mining
77 of *Pseudomonas*-borne recombinases from known protein families (i.e., Red β , ERF, GP2.5, SAK, and
78 SAK4; Lopes et al., 2010) followed by experimental validation of the most promising in a standardized
79 recombineering test exposed two new enzymes (Ssr and Rec2: Aparicio et al., 2016; Ricaurte et al.,
80 2018; Aparicio et al., 2020). These recombinases delivered a comparatively high level of activity in the
81 reference strains *P. putida* KT2440 and its genome-reduced derivative *P. putida* EM42. Still, numbers
82 were way below those reported for *E. coli*. Furthermore, the action of the endogenous MMR system of
83 this bacterium impeded single nucleotide changes (i.e., A to T, mismatch A:A) that were efficiently fixed
84 by the indigenous *mutS/mutL* device (Aparicio et al., 2016; Aparicio et al., 2019b).

85

86 In this work we have set out to overcome the bottlenecks to efficacious recombineering in *P. putida*
87 mentioned above. The approach builds on the apparently superior ability of the Rec2 recombinase to
88 promote DNA annealing with exogenous synthetic oligonucleotides during chromosomal replication. By
89 playing with a stringent expression system for *rec2*, applying multiple cycles of recombinase production/
90 oligonucleotide transformation and reversibly inhibiting the MMR system during a limited time window
91 we report below high-fidelity recombination frequencies that approach those achieved with the
92 archetypal Red-based system (Datsenko and Wanner, 2000). This opens genome-editing possibilities in

93 this environmental bacterium that were thus far limited to strains of *E. coli*, closely related enteric
94 species (Nyerges et al., 2018; Szili et al., 2019) and some lactic acid bacteria (van Pijkeren et al., 2012).

95

96 RESULTS AND DISCUSSION

97

98 *Optimization of Rec2 and MutL_{E36K}^{PP} delivery for ssDNA recombineering*

99

100 The bicistronic gene cassette of pSEVA2514-*rec2-mutL_{E36K}^{PP}* (Fig. 1) was developed earlier for
101 examining the hierarchy of recognition of different types of single nucleotide mispairs by the native
102 mismatch repair (MMR) system of *P. putida* (Aparicio et al., 2019b). During the course of that work, we
103 noticed that a short, transient, thermal induction of the Rec2 recombinase increased very significantly
104 ssDNA recombineering (~ 1 order of magnitude) as compared to the same with an expression device
105 responsive to 3-methyl-benzoate (i.e. *xy/S/Pm*). Although the reason for this improvement is not entirely
106 clear, it may have resulted from [i] the short-lived, high-level transcription of the otherwise toxic
107 recombinase—as compared to the permanent hyperexpression caused by the chemically-inducible
108 system, [ii] thermal inactivation of ssDNA nucleases and thus improved survival of the mutagenic
109 oligonucleotides *in vivo* or [iii] a combination of both. In any case, the average frequency of single-base
110 replacements in just one single-shot recombineering test was in the range of 1E⁻² mutants per viable
111 cell. This was high compared to previous recombineering efforts in this bacterium (Aparicio et al., 2016)
112 but still low for identifying mutations without a selectable phenotype. We however speculated that by
113 multi-cycling the procedure with short thermal pulses of induction/resetting of recombinase expression
114 and transformation with mutagenic oligos, such frequencies could be added at each cycle, eventually
115 resulting in high nucleotide replacement rates. A second realization of (Aparicio et al., 2019b) was that
116 transient co-expression of the dominant allele MutL_{E36K}^{PP} of the MMR system of *P. putida* along with the
117 *rec2* gene in plasmid pSEVA2514-*rec2-mutL_{E36K}^{PP}* (Fig. 1) virtually eliminated recognition of any type of
118 base mispairings in DNA. This allowed entering all classes of nucleotide replacements which would
119 otherwise be conditioned by MMR—without triggering a general mutagenic regime. Yet, note that both
120 activities (Rec2 and MutL_{E36K}^{PP}) were delivered *in vivo* with a high copy number vector with an origin or
121 replication (RSF1010) of unknown thermal sensitivity. This may result in some instability upon thermal
122 cycling of the procedure for boosting recombineering efficiency (see below). In order to determine the
123 best plasmid frame for *rec2-mutL_{E36K}^{PP}* transient expression, the cognate DNA segment was recloned in

124 vectors pSEVA2214 (RK2 origin or replication, low copy number) and pSEVA2314 (pBBR1 origin,
125 medium copy number) as shown in Fig. 1A. Recombineering tests were then carried out with
126 oligonucleotide NR, which generated a double mutation in *gyrA* endowing resistance to nalidixic acid
127 (Nal^R) by means of two MMR-sensitive changes G → A and C → T. In parallel, another MMR-
128 insensitive change A → C was also tested with oligonucleotide SR that mutated *rpsL* for making cells
129 resistant to streptomycin (Sm^R). The results of this test indicated pSEVA2314-*rec2-mutL*_{E36K}^{PP} as the
130 preferred construct of reference for the multi-site mutagenesis platform presented below. On the basis of
131 the above we set out to recreate in *P. putida* the same conditions that enabled implementation in *E. coli*
132 of high-efficiency ssDNA recombineering protocols such as MAGE (Wang et al., 2009), DiVERGE,
133 (Nyerges et al., 2018), and pORTMAGE (Nyerges et al., 2016)—and thus expand frontline genomic
134 editing methods towards that environmentally and industrially important bacterium.

135

136 *Cyclic pulses of rec2/mutL*_{E36K}^{PP} expression enable a high level of single-nucleotide substitutions

137

138 The first issue at stake was determining the frequencies of mutations caused by using a cocktail of
139 oligonucleotides targeting 5 genes representative of diverse genomic locations, different types of
140 nucleotide changes and associated or not to selectable traits upon multiple ssDNA recombineering
141 cycles. The genes at stake, their position in the chromosomal map, the cognate phenotypes and the
142 type of replacements brought about by the corresponding mutagenic ssDNAs are summarized in Fig. 2.
143 They were all designed to pair sequences in the lagging strand of the replication fork in each of the
144 replichores of the *P. putida* genome according to (Aparicio et al., 2016). Note that the experiments were
145 run with *P. putida* EM42, not with the archetypal strain KT2440. This is because it is a *recA*⁺ derivative
146 of the EM383 genome-streamlined variant that has higher endogenous levels of ATP and NAD(P)H and
147 has thus become a preferred metabolic engineering platform (Martinez-Garcia et al., 2014). Moreover,
148 the modifications entered in *P. putida* EM42 make this strain more tolerant to pulses of high-temperature
149 (Aparicio et al., 2019a), as repeatedly applied throughout this work (see below). The cyclic
150 recombineering protocol (see Transparent Methods for details) is summarized in Fig. 3, and it basically
151 involves four steps: [i] growing cells, [ii] triggering thermal induction of *rec2* and *mutL*_{E36K}^{PP} genes by a
152 short heat-shock, [iii] preparing competent cells for electroporation with the mutagenic oligonucleotides
153 and [iv] recovering the culture for a new cycle.

154 The results of applying multiple recombineering cycles to *P. putida* EM42 (pSEVA2314-*rec2-mutL*_{E36K}^{PP})
155 with the oligonucleotides listed in Fig. 2B are shown in Fig. 4A. Note that the frequencies of mutant
156 appearance increased during the runs from $2.8E^{-3}$ (1 cycle) \rightarrow $9.3E^{-2}$ (10 cycles) in the case of *gyrA*, to
157 $4.8E^{-2}$ \rightarrow $2.0E^{-1}$ for *pyrF* under the same conditions. In the best-case scenario (i.e. gene *rpsL*), the
158 frequencies multiplied by 24-fold, reaching a remarkable 21%. After the 10th cycle, these figures are
159 thus close to the rates reported in *E. coli* with the archetypal Red- β system of phage lambda and also to
160 the theoretical limit of recombineering frequencies (25 %) that stems from segregation of one allelic
161 change after two rounds of genome replication (Wang et al., 2009; Nyerges et al., 2016). It is worth to
162 mention that control strain *P. putida* EM42 harbouring insert less vector pSEVA2314—but transformed
163 with the same mutagenic oligonucleotides—gave rise to recombineering frequencies $\sim 1E^{-5}/1E^{-6}$
164 mutants/viable cells per cycle for single changes (Fig. S1). Given that these background levels are
165 higher with thermal induction than with chemical induction (Ricaurte et al., 2018), it is plausible that heat
166 shock intrinsically improves recombineering regardless of the action of heterologous recombinases. As
167 a matter of fact, purely endogenous ssDNA recombineering at significant frequencies has been reported
168 in a variety of Gram-negative bacteria, including *E. coli* and *Pseudomonas syringae* (Swingle et al.,
169 2010b), a fact that play in our favour for establishing the methodology in *P. putida*.

170

171 The most remarkable outcome of the operations shown in Fig. 4A was that such high figures enabled
172 manual screening of inconspicuous mutations, thus avoiding the need of adding a genetic
173 counterselection device (e.g., CRISPR/Cas9) for identifying rare changes. Since these results
174 accredited the value of multi-cycling thermoinduction of the bicistronic *rec2-mutL*_{E36K}^{PP} operon of
175 pSEVA2314-*rec2-mutL*_{E36K}^{PP} for raising ssDNA recombineering efficiency, the next obvious question
176 was whether the high figures could afford simultaneous multi-site genomic editing with mixtures of
177 mutagenic oligos, in a fashion reminiscent of the MAGE (Multiplex Automated Genome Engineering)
178 process available for *E. coli*.

179

180 *Multi-site editing of non-adjacent genomic locations*

181

182 Given average individual mutation rates of 10% after 10 thermal recombineering cycles and assuming
183 they are separately maintained when cells face a cocktail of mutagenic oligonucleotides one can predict
184 frequencies of 1% double changes all the way to 0.001 % mutants ($1E^{-5}$) of genomes with all the 5

185 changes in the absence of any phenotypic advantage. To test this prediction we subjected a culture of *P.*
186 *putida* EM42 (pSEVA2314-*rec2-mut*_{L_{E36K}^{PP}}) to 10 cycles of thermoinduced recombineering (see
187 Transparent Methods) with re-transformation in each cycle with an equimolar mixture of oligos SR, NR,
188 RR, PR and CR (Fig. 2B; Supplementary Table S1) so that all possible changes could be entered in the
189 same cells. Emergence of multiple (i.e. quadruple and quintuple) mutations in the population was then
190 monitored at cycles I, V and X and their frequencies recorded. Fig. 4B shows the results of such a
191 procedure. The data exposed a good match between the theoretical expectation of multiple changes
192 and the actual figures, although the evolution of the mutation rates was not linear. At cycle #1, single
193 changes showed recombineering frequencies barely below $1E^{-2}$ mutants per viable cell. If we take that
194 as a reference, theoretical frequencies acquisition of 4 and 5 changes would be $1E^{-8}$ and $1E^{-10}$
195 respectively, while actual numbers were way higher ($6E^{-6}$ and $2E^{-7}$). By cycle #5, single changes
196 reached average recombineering above $5E^{-2}$. The gross theoretical prediction for simultaneous
197 appearance of 4 and 5 changes would be as low as $6E^{-6}$ and $3E^{-7}$. Yet, again, the actual experiments
198 yield $1.3E^{-4}$ and $2.3E^{-6}$ mutants per viable cell for quadruple and quintuple mutants. By cycle #10,
199 however, the scenario was different. Single changes appeared at frequencies $\sim 1E^{-1}$, close to the
200 theoretical maximum of recombineering efficiency ($2.5 E^{-1}$). In this case, predicted frequencies for 4-5
201 changes ranged $1E^{-4}$ and $1E^{-5}$, which were very similar to the actual numbers delivered by the
202 experiment i.e. $2E^{-4}$ and $6E^{-6}$.

203

204 The results above suggested that, during the first 5 recombineering cycles a strong co-selection
205 phenomenon occurs. Appearance of multiple mutations fall 2-3 logs higher than expected, suggesting
206 that cells undergoing ssDNA incorporation in specific loci are more prone to incorporate changes in
207 other genomic locations. This phenomenon, which has been observed before (Carr et al., 2012;
208 Gallagher et al., 2014) could be due to differences in the ability of single cells in a population to uptake
209 exogenous ssDNA upon electroporation. Regardless of the specific mechanisms, the results of Fig. 4B
210 show that multi-cycle recombineering boosts mutagenic frequencies through single to quintuple
211 changes. Yet, while 10 cycles appear to reach saturation at single sites, it is plausible that additional
212 runs could enrich further the population in multi-edited bacterial cells. Taken together, the experiments
213 of Fig. 4 document the power of the hereby described method for simultaneously targeting 5 genomic
214 sites of *P. putida* for desired mutations. On this basis we propose to call the entire workflow High-
215 Efficiency Multi-site Genomic Editing (or HEMSE). The method is conceptually comparable to Multiple

216 Automated Genome Editing developed for *E. coli* (MAGE, (Wang et al., 2009)) but it lacks (thus far) the
217 automation aspect.

218

219 Since a growing culture of *P. putida* in LB typically ranges 10^8 - 10^9 cells/ml from early exponential to
220 early stationary phase, we speculated that the maximum number of genes that could be edited in an
221 HEMSE experiment of this sort with mixed oligos in the absence of any selective advantage or
222 phenotypic screening could be ~ 8-9. This is clearly not enough for massive changes of the sort
223 necessary for e.g. recoding a whole genome (Isaacs et al., 2011) or reassigning/erasing specific triplets
224 (Ostrov et al., 2016). Fortunately, in most typical metabolic engineering endeavours, the issue is not so
225 much entering many defined mutations in given chromosomal sites but fostering the system to explore a
226 solution space by letting it come up with many combinations—the most successful of which can be
227 enriched and subject to further mutation rounds. This effect can be exacerbated if the mutagenic oligos
228 boost the diversification of e.g. regulatory sequences, so their combination generates fluctuations in the
229 stoichiometry of a multi-gene pathway (Hueso-Gil et al., 2019) —or they create variants of the same
230 protein with different activities by diversifying specific segments. The technical issue shared by all these
231 scenarios is the focusing of the diversification in a defined sequence window of the genomic DNA. In
232 this context the question is whether the above described HEMSE is instrumental to this end also—as
233 the recombineering-based method to the same end called DIVERGE is in *E. coli* and related
234 enterobacteria (Nyerges et al., 2018).

235

236 *Diversification of the SD motif context creates new functional RBSs in P. putida*

237

238 In order to have a tractable proxy of generation *in vivo* of large libraries of functional DNA sequences in
239 the *P. putida* genome, the experimental setup shown in Fig. 5 was developed. In it, a Tn7 mini-
240 transposon vector was inserted with the *gfp* gene downstream of the constitutive promoter P_{EM7} but
241 lacking a recognizable Shine Dalgarno (SD) sequence for translation initiation. The hybrid transposon
242 was subsequently inserted in the cognate *attTn7* site of the *P. putida* EM42 chromosome (see
243 Transparent Methods) from which it was expectedly unable to produce any detectable fluorescence.
244 The resulting strain (*P. putida* TA245, Supplementary Table S2) was transformed with pSEVA2314-*rec2*-
245 *mutL*_{E36K}^{PP} and used in recombineering experiments with oligonucleotides designed for creating RBS
246 variants. The business parts of such oligonucleotides are shown in Fig. 5B. As controls we used oligos

247 named RBS-C₆ and RBS-C₉. These ssDNA enter respectively a short or an extended Shine-Dalgarno
248 (SD) sequence, 8 bp upstream of the start codon of the *gfp* gene using as a reference the *P. putida* 16S
249 ribosomal gene containing the core for optimal translation 5'-GAGG-3' (Shine and Dalgarno, 1975;
250 Kozak, 1983; Farasat et al., 2014). For RBS diversification we used oligonucleotides RBS-Deg₆ and RBS-
251 Deg₉ (Fig. 5B), which include soft randomized sequences with discrete changes R (A or G) that cover 6
252 degenerated positions with a potential to generate 64 (= 2⁶) combinations. This was expected to create
253 a large population of RBS of different efficacies, which could be quantified through fluorescent emission
254 of individual cells.

255

256 For the experiments described below, *P. putida* TA245 (pSEVA2314-*rec2-mut*_{E36K}^{PP}) was separately
257 subject to one recombineering cycle with each of four oligos of Fig. 5B, after which cells were diluted
258 and plated in charcoal-LB agar for easing visual detection of colonies emitting low fluorescence on a
259 black background. Positive controls RBS-C₆ and RBS-C₉ allowed the estimation of editing frequencies as
260 GFP⁺ cells/total number of cells, which resulted in 5.9E⁻⁴ and 9.9E⁻⁴, respectively. Those values were
261 relatively low as compared to the recombineering efficiencies reported above for single changes (~ 1E-
262 2). This could be possibly due to the shorter homology arms the oligos (30 nt) and the extended
263 sequence inserted between them (Aparicio et al., 2020). Yet, these figures provided a reference for
264 subsequent quantification of the effect of soft-randomized oligos RBS-Deg₆ and RBS-Deg₉. After
265 treatment with these last, cultures were diluted and plated for inspection of ~ 9000 colonies resulting of
266 each recombineering experiment. Visual screening of the colonies revealed the appearance of 67 and
267 53 fluorescent clones coming, respectively, from experiments with RBS-Deg₆ and RBS-Deg₉. These 120
268 clones were picked up for further analysis. PCR and sequencing of the region upstream the *gfp* gene
269 allowed identification of 14 variants of RBS-Deg₆ and 17 variants of RBS-Deg₉, the GFP levels of which
270 were measured by flow cytometry. The results plotted in Fig. 6 show that the different variants delivered
271 emissions ranging from very low to high fluorescent levels across a 20-fold change span. It is worth to
272 highlight that the best RBS of the series (Strain Code #33, Fig. 6) has a perfect match with the
273 complementary sequence of the last 9 nt of the 16S ribosomal RNA of *P. putida* (PP_16SA). Other
274 clones (e.g. #32; RBS = 5'-AAGGAG-3') displayed also high fluorescence levels. Interestingly, a few
275 productive variants contained the same 6-nt sequence in the degenerated region regardless of the type
276 of randomized oligo (e.g. #32 = #30, #26 = #16, #14 = #11 and #23 = #10). While most of the high-
277 signal variants belong to the longer RBS-C₉-borne clones, the comparison of signals does not support

278 the hypothesis that longer complementarity to the 16s ribosomal sequence correlates with more efficient
279 translation. Other factors have been proposed to affect translation efficacy of RBS variants, such as the
280 stability and secondary structure of RNA and transcriptional efficiency (Chen et al., 1994; Salis et al.,
281 2009). Regardless of the possible biological significance of the results, the data of Fig. 6 certifies the
282 efficacy of the HEMSE platform to generate diversity in specific genomic segments—a welcome feature
283 which can doubtless be multiplexed to other chromosomal locations as required.

284

285 *Conclusion*

286

287 In this work we have merged and adapted to *P. putida* and in a single platform 3 of the most efficacious
288 genetic tools available to metabolic engineers for generating diversity *in vivo* focused into a
289 predetermined number of chromosomal DNA segments: ssDNA recombineering (Wang et al., 2009),
290 portable MAGE (Nyerges et al., 2016) and DivERGE (Nyerges et al., 2018). Although conceptually
291 identical to such methods already applied to *E. coli*, their recreation in a non-enterobacterial species
292 involved [i] the search and testing of functional equivalents of the parts involved but recruited from
293 *Pseudomonas* genomes and [ii] adaptation and optimization to the distinct physiology of the species
294 and strain at stake. While we have not made a side-by-side comparison of the frequencies resulting
295 from standard MAGE in *E. coli* and the ones presented in this work, numbers in the range of 10%
296 replacements after 10 recombineering cycles could be sufficient to implement the same powerful
297 method in *P. putida*. We are reluctant, however, to use the same acronym, because the automation
298 feature is not in sight and the multiplexing still problematic with the current efficiencies.

299

300 One can envision various ways through which HEMSE could be further improved. End-terminal
301 degradation of the mutagenic oligos *in vivo* does not seem to be an issue: performance of 5'-
302 phosphorothioated ssDNA (which cannot be degraded by exonucleases (Wang et al., 2009) is
303 indistinguishable from non-phosphorothioated equivalents (Aparicio et al., 2020). However, the nature
304 and origin of the recombinase that catalyzes invasion of the DNA replication fork by the synthetic oligo
305 makes a considerable difference (Chang et al., 2019). It is possible that such recombinases act in
306 concert with additional endogenous proteins that could be characteristic of each species (Caldwell et al.,
307 2019; Yin et al., 2019). It seems thus desirable that future alternatives to the Rec2 activity encoded in
308 pSEVA2314-*rec2-mut*_{L_{E36K}}^{PP} (Fig. 1) are mined in *Pseudomonas* genomes and phages—by themselves

309 or in combination with other complementary genes. It should be straightforward to then replace the *rec2*
310 of pSEVA2314-*rec2-mut*_{L_{E36K}}^{PP} by the improved counterparts, should they appear, while maintaining
311 the rest of the hereby described HEMSE pipeline.

312

313 METHODS

314

315 All detailed methods can be found in the accompanying **Transparent Methods** in the Supplemental
316 Information File

317

318 SUPPLEMENTAL INFORMATION

319 Supplemental Information can be found in the attached File

320

321 ACKNOWLEDGMENTS

322 Authors are indebted to Sebastian S. Cocioba for posting in Twitter the useful recipe of LB-charcoal
323 medium (<https://twitter.com/ATinyGreenCell/status/1037332606432555009>) and to Csaba Pal (Institute
324 of Biochemistry, Biological Research Centre, Szeged) for his continued support. This work was funded
325 by the MADONNA (H2020-FET-OPEN-RIA-2017-1-766975), BioRoboost (H2020-NMBP-BIO-CSA-
326 2018), and SYN BIO4FLAV (H2020-NMBP/0500) Contracts of the European Union and the S2017/BMD-
327 3691 InGEMICS-CM funded by the Comunidad de Madrid (European Structural and Investment Funds).

328

329 AUTHOR CONTRIBUTIONS

330 TA, EMG, AN and VdL designed the study. TA run the experiments. TA, EMG and VdL wrote the
331 manuscript.

332

333 DECLARATION OF INTERESTS

334 Authors declare no conflict of interest

335

336

337 REFERENCES

338

339 Aparicio, T., de Lorenzo, V., and Martínez-García, E. (2019a) Improved Thermotolerance of Genome-
340 Reduced *Pseudomonas putida* EM42 Enables Effective Functioning of the P_L /cl857 System.
341 *Biotechnol J* **14**: e1800483.

342 Aparicio, T., de Lorenzo, V., and Martínez-García, E. (2020) A Broad Host Range Plasmid-Based
343 Roadmap for ssDNA-Based Recombineering in Gram-Negative Bacteria. In *Horizontal Gene*
344 *Transfer: Methods and Protocols*. de la Cruz, F. (ed). New York, NY: Springer US, pp. 383-398.

345 Aparicio, T., Jensen, S.I., Nielsen, A.T., de Lorenzo, V., and Martínez-García, E. (2016) The Ssr protein
346 (T1E_1405) from *Pseudomonas putida* DOT-T1E enables oligonucleotide-based recombineering
347 in platform strain *P. putida* EM42. *Biotechnol J* **11**: 1309-1319.

348 Aparicio, T., Nyerges, A., Nagy, I., Pal, C., Martínez-García, E., and de Lorenzo, V. (2019b) Mismatch
349 repair hierarchy of *Pseudomonas putida* revealed by mutagenic ssDNA recombineering of the
350 *pyrF* gene. *Environ Microbiol* doi:10.1111/1462-2920.14814.

351 Bao, Z., Cartinhour, S., and Swingle, B. (2012) Substrate and target sequence length influence
352 RecTE(P_{sy}) recombineering efficiency in *Pseudomonas syringae*. *PLoS One* **7**: e50617.

353 Caldwell, B.J., Zakharova, E., Filsinger, G.T., Wannier, T.M., Hempfling, J.P., Chun-Der, L. et al. (2019)
354 Crystal structure of the Redbeta C-terminal domain in complex with lambda Exonuclease reveals
355 an unexpected homology with lambda Orf and an interaction with *Escherichia coli* single stranded
356 DNA binding protein. *Nucleic Acids Res* **47**: 1950-1963.

357 Carr, P.A., Wang, H.H., Sterling, B., Isaacs, F.J., Lajoie, M.J., Xu, G. et al. (2012) Enhanced multiplex
358 genome engineering through co-operative oligonucleotide co-selection. *Nucleic Acids Res* **40**:
359 e132.

360 Chang, Y., Wang, Q., Su, T., and Qi, Q. (2019) The efficiency for recombineering is dependent on the
361 source of the phage recombinase function unit. *bioRxiv*: 745448.

362 Chen, H., Bjerknes, M., Kumar, R., and Jay, E. (1994) Determination of the optimal aligned spacing
363 between the Shine-Dalgarno sequence and the translation initiation codon of *Escherichia coli*
364 mRNAs. *Nucleic Acids Res* **22**: 4953-4957.

365 Chen, W., Zhang, Y., Zhang, Y., Pi, Y., Gu, T., Song, L. et al. (2018) CRISPR/Cas9-based genome
366 editing in *Pseudomonas aeruginosa* and cytidine deaminase-mediated base editing in
367 *Pseudomonas* species. *iScience* **6**: 222-231.

- 368 Costantino, N., and Court, D.L. (2003) Enhanced levels of lambda Red-mediated recombinants in
369 mismatch repair mutants. *Proc Natl Acad Sci USA* **100**: 15748-15753.
- 370 Datsenko, K.A., and Wanner, B.L. (2000) One-step inactivation of chromosomal genes in *Escherichia*
371 *coli* K-12 using PCR products. *Proc Natl Acad Sci USA* **97**: 6640-6645.
- 372 Ellis, H.M., Yu, D., DiTizio, T., and Court, D.L. (2001) High efficiency mutagenesis, repair, and
373 engineering of chromosomal DNA using single-stranded oligonucleotides. *Proc Natl Acad Sci*
374 *USA* **98**: 6742-6746.
- 375 Farasat, I., Kushwaha, M., Collens, J., Easterbrook, M., Guido, M., and Salis, H.M. (2014) Efficient
376 search, mapping, and optimization of multi-protein genetic systems in diverse bacteria. *Mol Syst*
377 *Biol* **10**: 731.
- 378 Gallagher, R.R., Li, Z., Lewis, A.O., and Isaacs, F.J. (2014) Rapid editing and evolution of bacterial
379 genomes using libraries of synthetic DNA. *Nat Protoc* **9**: 2301-2316.
- 380 Hueso-Gil, A., Nyerges, Á., Pál, C., Calles, B., and de Lorenzo, V. (2019) Multiple-site diversification of
381 regulatory sequences enables inter-species operability of genetic devices. *bioRxiv*: 771782.
- 382 Isaacs, F.J., Carr, P.A., Wang, H.H., Lajoie, M.J., Sterling, B., Kraal, L. et al. (2011) Precise
383 manipulation of chromosomes in vivo enables genome-wide codon replacement. *Science* **333**:
384 348-353.
- 385 Jiang, W., Bikard, D., Cox, D., Zhang, F., and Marraffini, L.A. (2013) RNA-guided editing of bacterial
386 genomes using CRISPR-Cas systems. *Nat Biotechnol* **31**: 233-239.
- 387 Kozak, M. (1983) Comparison of initiation of protein synthesis in procaryotes, eucaryotes, and
388 organelles. *Microbiol Rev* **47**: 1-45.
- 389 Lesic, B., and Rahme, L.G. (2008) Use of the lambda Red recombinase system to rapidly generate
390 mutants in *Pseudomonas aeruginosa*. *BMC Mol Biol* **9**: 20.
- 391 Liang, R., and Liu, J. (2010) Scarless and sequential gene modification in *Pseudomonas* using PCR
392 product flanked by short homology regions. *BMC Microbiol* **10**: 209.
- 393 Lopes, A., Amarir-Bouhram, J., Faure, G., Petit, M.-A., and Guerois, R. (2010) Detection of novel
394 recombinases in bacteriophage genomes unveils Rad52, Rad51 and Gp2. 5 remote homologs.
395 *Nucleic Acids Res* **38**: 3952-3962.

- 396 Luo, X., Yang, Y., Ling, W., Zhuang, H., Li, Q., and Shang, G. (2016) *Pseudomonas putida* KT2440
397 markerless gene deletion using a combination of lambda Red recombineering and Cre/loxP site-
398 specific recombination. *FEMS Microbiol Lett* **363**(4) pii: fnw014
- 399 Martínez-García, E., Nikel, P.I., Aparicio, T., and de Lorenzo, V. (2014) *Pseudomonas* 2.0: genetic
400 upgrading of *P. putida* KT2440 as an enhanced host for heterologous gene expression. *Microb*
401 *Cell Fact* **13**: 159.
- 402 Martínez-García, E., and de Lorenzo, V. (2019) *Pseudomonas putida* in the quest of programmable
403 chemistry. *Curr Op Biotech* **59**: 111-121.
- 404 Nikel, P.I., Martínez-García, E., and De Lorenzo, V. (2014) Biotechnological domestication of
405 pseudomonads using synthetic biology. *Nature Revs Microbiol* **12**: 368-379.
- 406 Nikel, P.I., Chavarria, M., Danchin, A., and de Lorenzo, V. (2016) From dirt to industrial applications:
407 *Pseudomonas putida* as a synthetic biology chassis for hosting harsh biochemical reactions. *Curr*
408 *Op Chem Biol* **34**: 20-29.
- 409 Nyerges, A., Csorgo, B., Nagy, I., Latinovics, D., Szamecz, B., Posfai, G., and Pal, C. (2014)
410 Conditional DNA repair mutants enable highly precise genome engineering. *Nucleic Acids Res*
411 **42**: e62.
- 412 Nyerges, A., Csorgo, B., Nagy, I., Balint, B., Bihari, P., Lazar, V. et al. (2016) A highly precise and
413 portable genome engineering method allows comparison of mutational effects across bacterial
414 species. *Proc Natl Acad Sci USA* **113**: 2502-2507.
- 415 Nyerges, A., Csorgo, B., Draskovits, G., Kintses, B., Szili, P., Ferenc, G. et al. (2018) Directed evolution
416 of multiple genomic loci allows the prediction of antibiotic resistance. *Proc Natl Acad Sci USA*
417 **115**: E5726-E5735.
- 418 Oesterle, S., Wuethrich, I., and Panke, S. (2017) Toward genome-based metabolic engineering in
419 bacteria. *Adv Appl Microbiol* **101**: 49-82.
- 420 Ostrov, N., Landon, M., Guell, M., Kuznetsov, G., Teramoto, J., Cervantes, N. et al. (2016) Design,
421 synthesis, and testing toward a 57-codon genome. *Science* **353**: 819-822.
- 422 Ricaurte, D.E., Martínez-García, E., Nyerges, A., Pal, C., de Lorenzo, V., and Aparicio, T. (2018) A
423 standardized workflow for surveying recombinases expands bacterial genome-editing capabilities.
424 *Microb Biotechnol* **11**: 176-188.
- 425 Ronda, C., Pedersen, L.E., Sommer, M.O., and Nielsen, A.T. (2016) CRMAGE: CRISPR optimized
426 mage recombineering. *Sci Repts* **6**: 19452.

- 427 Salis, H.M., Mirsky, E.A., and Voigt, C.A. (2009) Automated design of synthetic ribosome binding sites
428 to control protein expression. *Nat Biotechnol* **27**: 946-950.
- 429 Shine, J., and Dalgarno, L. (1975) Determinant of cistron specificity in bacterial ribosomes. *Nature* **254**:
430 34-38.
- 431 Swingle, B., Bao, Z., Markel, E., Chambers, A., and Cartinhour, S. (2010a) Recombineering using
432 RecTE from *Pseudomonas syringae*. *Appl Environ Microbiol* **76**: 4960-4968.
- 433 Swingle, B., Markel, E., Costantino, N., Bubunencko, M.G., Cartinhour, S., and Court, D.L. (2010b)
434 Oligonucleotide recombination in Gram-negative bacteria. *Mol Microbiol* **75**: 138-148.
- 435 Szili, P., Draskovits, G., Révész, T., Bogar, F., Balogh, D., Martinek, T. et al. (2019) Rapid evolution of
436 reduced susceptibility against a balanced dual-targeting antibiotic through stepping-stone
437 mutations. *Antimicrob Agents Chemother* **63**(9): pii: e00207-19.
- 438 van Pijkeren, J.-P., Neoh, K.M., Sirias, D., Findley, A.S., and Britton, R.A. (2012) Exploring optimization
439 parameters to increase ssDNA recombineering in *Lactococcus lactis* and *Lactobacillus reuteri*.
440 *Bioengineered* **3**: 209-217.
- 441 Wang, H.H., Isaacs, F.J., Carr, P.A., Sun, Z.Z., Xu, G., Forest, C.R., and Church, G.M. (2009)
442 Programming cells by multiplex genome engineering and accelerated evolution. *Nature* **460**: 894-
443 898.
- 444 Yin, J., Zheng, W., Gao, Y., Jiang, C., Shi, H., Diao, X. et al. (2019) Single-Stranded DNA-Binding
445 Protein and Exogenous RecBCD Inhibitors Enhance Phage-Derived Homologous Recombination
446 in *Pseudomonas*. *iScience* **14**: 1-14.
- 447 Yu, D., Ellis, H.M., Lee, E.C., Jenkins, N.A., Copeland, N.G., and Court, D.L. (2000) An efficient
448 recombination system for chromosome engineering in *Escherichia coli*. *Proc Natl Acad Sci USA*
449 **97**: 5978-5983.

450

451

FIGURES

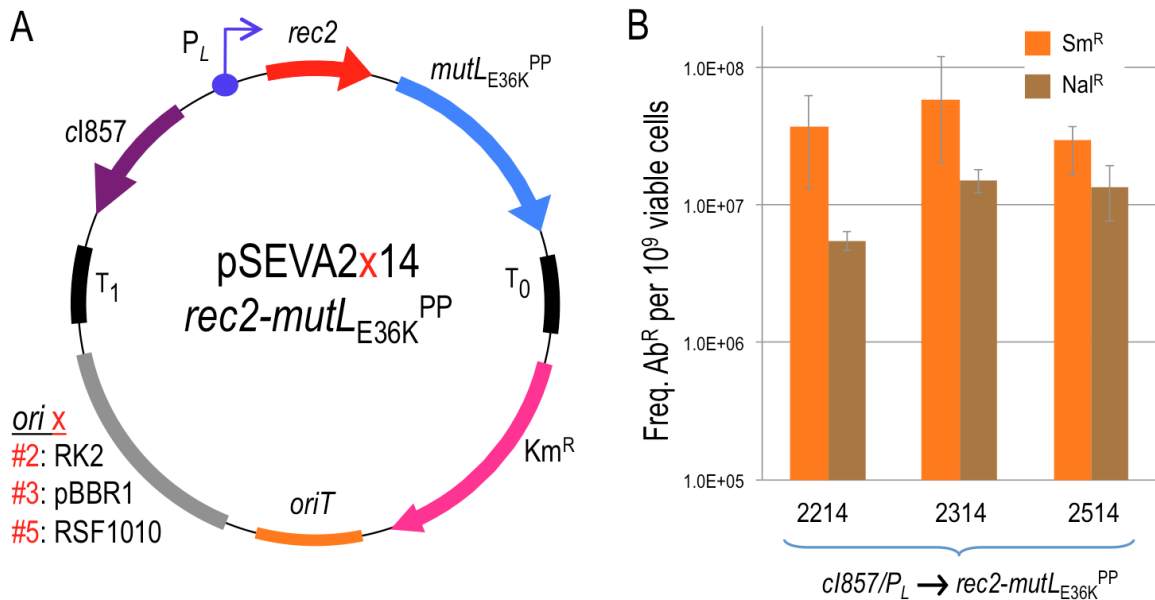
452

453

454 **Figure 1.** Influence of plasmid copy number in the editing efficiency of the heat-induced *rec2-mutL_{E36K}^{PP}*

455 genes

456



457

458

459 **A)** Genetic map and structure of plasmids used in this study. The figure shows the plasmids tested, all

460 having the same elements with the exception of the origin of replication, represented with "x". T₀ and T₁,

461 transcriptional terminators; Km, Kanamycin resistance gene; *oriT*, origin of transfer; cl857-P_L,

462 temperature inducible expression system; *rec2*, recombinase; *mutL_{E36K}^{PP}*, dominant-negative allele of

463 *mutL*; *ori x* (origin of replication): #2, RK2 (low copy number); #3, pBBR1 (medium copy number); #5,

464 RSF1010 (medium-high copy number). Pictures are not drawn to scale. **B)** Recombineering assays with

465 *P. putida* EM42: the strain harbouring each pSEVA2x14-*rec2-mutL_{E36K}^{PP}* variant was subjected to

466 recombineering with oligos SR and NR upon heat induction of the cl857-P_L expression system. After

467 overnight recovery, culture dilutions were plated on LB-Sm (SR oligo) and LB-Nal (NR oligo) to estimate

468 the number of allelic changes. Culture dilutions plated on LB allowed viable cells counting. Column

469 values represent mean recombineering frequencies (mutants per 10⁹ viable cells) of two independent

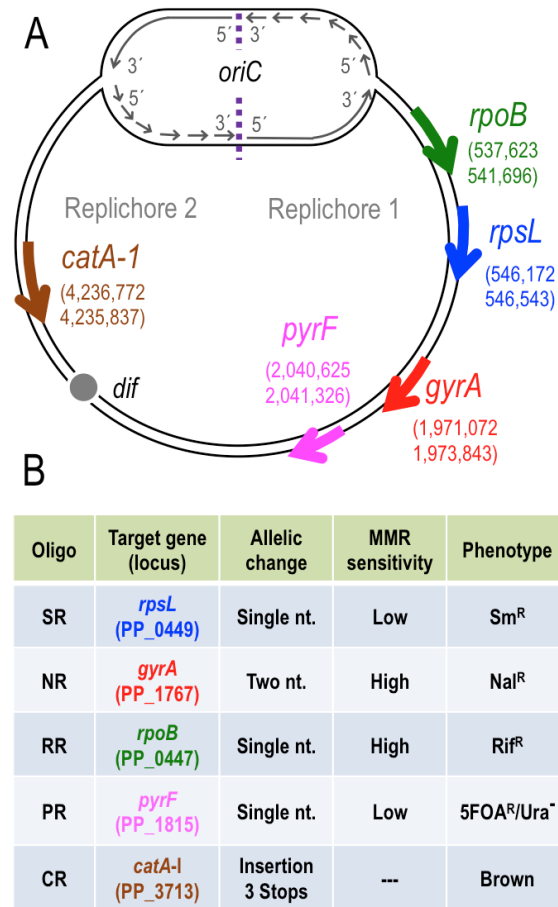
470 experiments with the standard deviation.

471

472

473 **Figure 2.** Target genes and recombining oligonucleotides used for HEMSE

474



475

476

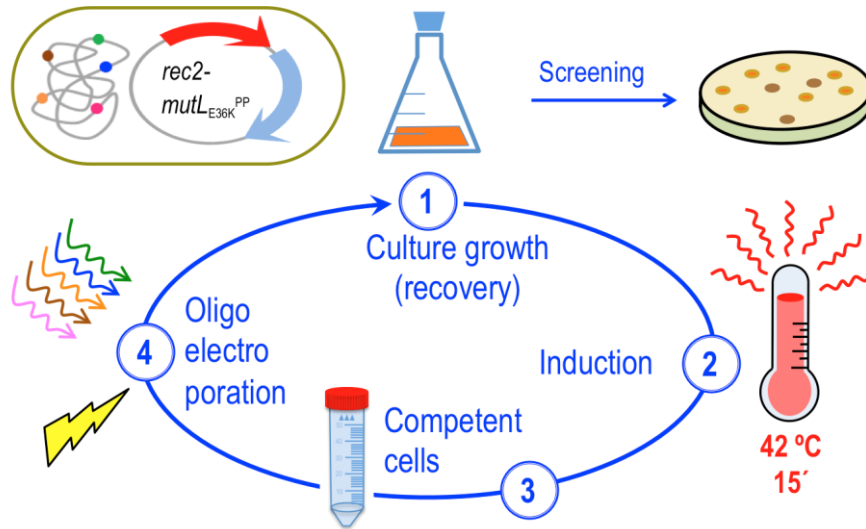
477 **A)** The 5 genes selected as targets for recombineering are represented in the chromosomal map of *P.*
 478 *putida* KT2440 with gene coordinates and strand orientation. *oriC* and *dif* regions are shown to define
 479 the two replichores in the genomic map. Pictures are not drawn to scale. **B)** The main features of
 480 recombineering oligonucleotides used to assay HEMSE are shown: name of oligo, target gene with its
 481 locus tag, type of allelic replacement, level of Mismatch Repair (MMR) sensitivity of the allelic changes
 482 and the cognate phenotypes produced. See Supplementary Tables S1 and S3 for additional
 483 information.

484

485

486 **Figure 3.** Scheme of HEMSE cycle

487



488

489

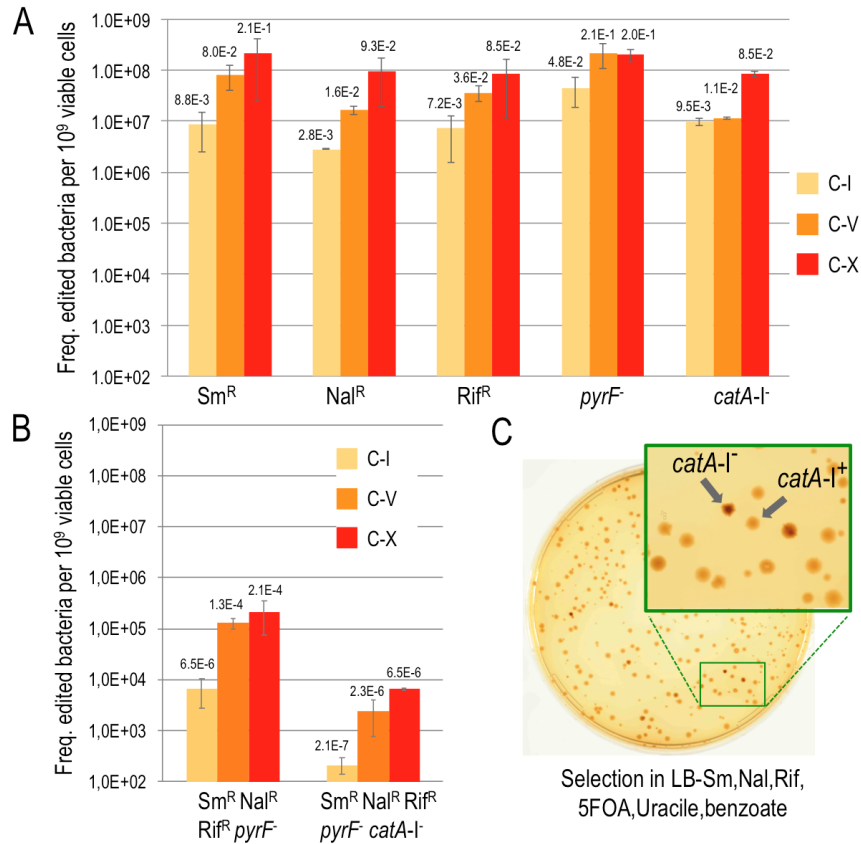
490 The main steps of the procedure are depicted: cultures of *P. putida* EM42 (pSEVA2314-*rec2-*
491 *mutL*_{E36K}^{PP}) grown at OD₆₀₀ = 1.0 are induced by a heat-shock at 42 °C/ 15 minutes, then competent
492 cells are prepared and transformed with recombineering oligonucleotides. After recovery on fresh media
493 at 30 °C/ 170 rpm, cultures enter in the next round of HEMSE by applying the induction step. Screening
494 of allelic replacements within a given cycle is performed after recovery by plating culture dilutions on the
495 appropriate solid media (see Transparent Methods for details)

496

497

498 **Figure 4. Editing efficiencies HEMSE**

499



500

501

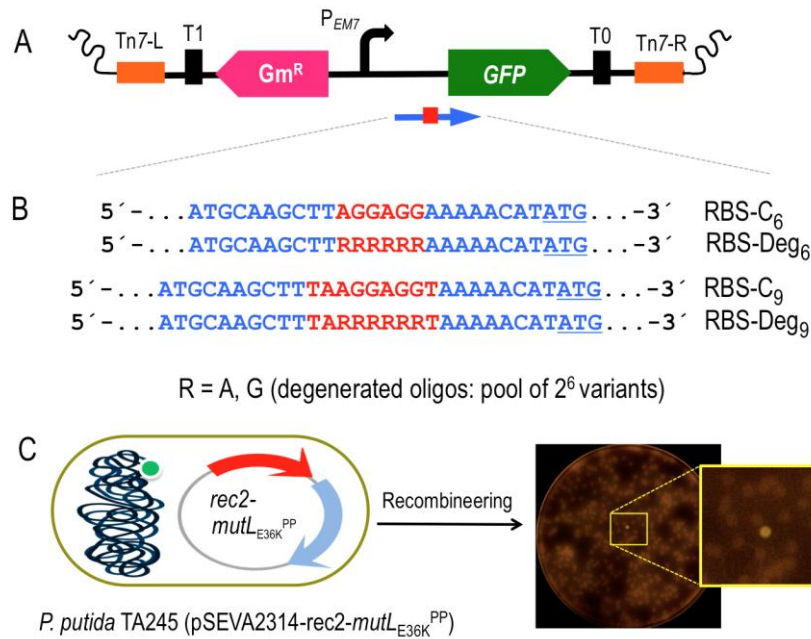
502 **A)** Editing efficiencies of single changes were assayed applying 10 cycles of HEMSE to *P. putida* EM42
 503 (pSEVA2314-*rec2-mutLE36k^{PP}*) using an equimolar mixture of oligos SR, NR, RR, PR and CR. After
 504 recovery steps of cycles n^o 1 (C-I), n^o 5 (C-V) and n^o 10 (C-X), appropriate dilutions of the cultures were
 505 plated on LB to estimate viable cells and also on LB solid media supplemented with Sm, Nal, Rif, 5FOA-
 506 Ura or benzoate to enumerate allelic replacements. Colonies growing on Sm, Nal, Rif or 5FOA-Ura were
 507 counted as allelic changes, while brown - catechol accumulating- colonies growing in LB-benzoate were
 508 counted as *catA*^{-I} clones. Recombineering frequencies of single replacements at each cycle were
 509 normalized to 10⁹ viable cells and the medias of two independent replicas were plotted with standard
 510 deviations. Absolute recombineering frequencies (mutants per viable cell) are also depicted over the
 511 bars. **B)** From the same experiments explained above, editing efficiencies of multiple changes were
 512 analysed. Dilutions of C-I, C-V and C-X were plated on LB-SmNalRif-5FOA-Ura and LB-SmNalRif-
 513 5FOA-Ura-benzoate solid media, allowing the estimation of, respectively, quadruple (Sm^R Nal^R Rif^R
 514 *pyrF*⁻) and quintuple (Sm^R Nal^R Rif^R *pyrF*⁻ *catA*^{-I}) editions. Results were represented as in A). **C)** A
 515 representative plate of quintuple screening at C-X is shown. The zoom-up shows colonies with the
 516 characteristic dark-brown phenotype of *catA*^{-I} clones.

517

518

519 **Figure 5.** Diversification of the *gfp* Shine Dalgarno motif

520



521

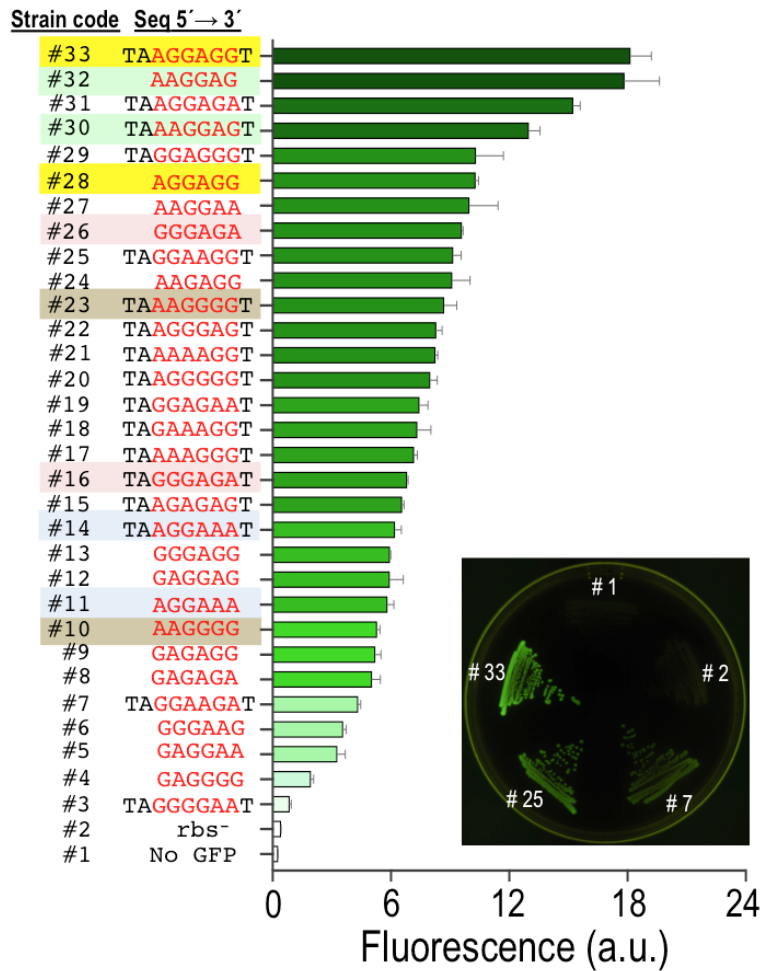
522

523 **A)** A mini-Tn7 transposon bearing the *gfp* gene devoid of its original SD sequence and under the control
 524 of the constitutive *P*_{EM7} promoter was constructed. The elements depicted are: Tn7-L and Tn7-R, left
 525 and right Tn7 sites; T₀ and T₁, transcriptional terminators; Gm^R, Gentamicin resistance gene; *P*_{EM7},
 526 constitutive promoter; GFP, Green Fluorescent Protein gene. A blue arrow represents the target region
 527 of recombineering oligonucleotides aimed to reconstruct the *gfp* ribosome binding site (shown as a red
 528 square). **B)** Partial sequence of the four recombineering oligonucleotides (Supplementary Table S1)
 529 designed to introduce SD motifs upstream the *gfp* gene. RBS-C₆ and RBS-C₉ insert, respectively,
 530 the semi-canonical AGGAGG and the canonical TAAGGAGGT SD motifs eight nucleotides upstream the
 531 ATG start codon of the *gfp* (underlined). RBS-Deg₆ and RBS-Deg₉ insert the randomized sequences
 532 RRRRRR and TARRRRRT, where R stands for A (adenine) or G (guanine). Each degenerated
 533 oligonucleotide comprises a pool of 64 variants (2⁶) with all possible combinations A/G. **C)** The mini-Tn7
 534 device was inserted in the *attTn7* site of *P. putida* EM42. Upon transformation with pSEVA2314-*rec2-*
 535 *mutL*_{E36K}^{PP}, the resulting strain *P. putida* TA245 (pSEVA2314-*rec2-mutL*_{E36K}^{PP}) was subjected to one
 536 HEMSE cycle with the recombineering oligos in independent experiments. After plating in LB-GmKm-
 537 charcoal, GFP positive clones were identified. A plate from the screening of RBS-Deg₉ is also shown, with
 538 a magnification of a fluorescent colony.

539

540 **Figure 6. Characterization of the diversified library of SD sequences**

541



542

543

544 The screening of the HEMSE experiments performed in *P. putida* TA245 (pSEVA2314-*rec2-mutL*_{E36K}^{PP})
545 with RBS-Deg₆ and RBS-Deg₉ yielded 31 variants in the ribosome binding site of the *gfp* gene. The GFP
546 expression of this library was analysed by flow cytometry including two negative controls: *P. putida*
547 EM42 (Strain #1), in which there is no *gfp* gene, and also the ancestral strain *P. putida* TA245
548 (pSEVA2314-*rec2-mutL*_{E36K}^{PP}), harbouring the mini-Tn7 and the *gfp* gene but lacking the original SD
549 sequence (Strain #2). The plot shows the mean fluorescent emission of individual clones from two
550 biological replicas with standard deviations. A Strain Code was assigned to each variant analysed and
551 the putative SD sequence identified 8 nt upstream the *gfp* start codon is shown. Variants showing
552 identical sequence in the randomized region are highlighted with the same color. A plate of LB-charcoal
553 agar with streaks of the two controls and three representative clones exhibiting low-, medium and high
554 signal rates (#7, #25 and #33, respectively) is also depicted under UV light.

SUPPLEMENTARY INFORMATION

TRANSPARENT METHODS

Strains and media

The bacterial strains employed in this study are listed in Supplementary Table S2. *E. coli* and *P. putida* strains were grown in liquid LB with shaking (170 rpm) at 37 °C and 30 °C, respectively (Sambrook et al., 1989) with the exception of *E. coli* strains bearing SEVA plasmids endowed with the cl857- P_L thermo-inducible expression system (cargo #14; i.e. pSEVA2514-*rec2-mutL*_{E36K^{PP}} and derivatives), which were grown at 30 °C to avoid promoter activation. After electroporation recovery during recombineering experiments was performed in Terrific Broth without glycerol (TB: 12 g l⁻¹ tryptone, 24 g l⁻¹ yeast extract, 2 g l⁻¹ KH₂PO₄, 9.4 g l⁻¹ K₂HPO₄). M9 minimal media was prepared according to (Sambrook et al., 1989). Solid media was prepared adding 15 g/L⁻¹ of agar to liquid media. M9 solid media was supplemented with 0.2% (w/v) citrate and appropriate antibiotics to select *P. putida* cells in mating experiments. Liquid and solid media were added, when necessary, with 50 µg ml⁻¹ of kanamycin (Km), 15 µg ml⁻¹ of gentamicin (Gm) for *P. putida* and 10 µg ml⁻¹ of the same antibiotic for *E. coli*, 30 µg ml⁻¹ of chloramphenicol (Cm), 100 µg ml⁻¹ of streptomycin (Sm), 100 µg ml⁻¹ of rifampicin (Rif), 50 µg ml⁻¹ of nalidixic acid (Nal), 20 µg ml⁻¹ of Uracil (Ura), 250 µg ml⁻¹ of 5-fluoroorotic acid (5-FOA) and 5 mM of benzoic acid (pH 11). For screening of fluorescent colonies, LB solid media was prepared with 1 mg ml⁻¹ of activated charcoal (Sigma-Aldrich Ref. C9157-500G) in order to better discriminate low-signal colonies. Activated charcoal was added to the LB-Agar prior autoclaving and the media poured into 150 mm Petri dishes after vigorous shaking to evenly distribute the insoluble charcoal particles.

General procedures, primers and bacterial transformation

Standard DNA manipulations were carried out following routine protocols (Sambrook et al., 1989) and according to manufacturer recommendations. Isothermal Assembly was performed with Gibson Assembly® Master Mix (New England Biolabs, Ipswich, MA, USA). Plasmidic DNA was

32 purified with the QIAprep® Spin Miniprep Kit, both purchased from Qiagen (Valencia, CA, USA).
33 DNA Amplitools Master Mix (Biotools, Madrid, Spain) was used for diagnosis PCRs and
34 amplification of DNA fragments for cloning purposes was done with Q5 polymerase (New
35 England Biolabs, Ipswich, MA, USA). Synthetic oligonucleotides used in this study are listed in
36 Supplementary Table S1 and were purchased from Sigma-Aldrich (St. Louis, MO, USA). PCR
37 products were purified with the Nucleospin® Gel and PCR Clean-up Kit (Macherey-Nagel,
38 Düren, Germany). DNA sequencing was performed in Macrogen (Spain). Transformation of *E.*
39 *coli* strains was carried out with chemically competent cells using the CaCl₂ method (Sambrook et
40 al., 1989). Plasmids were introduced in *P. putida* strains via tripartite mating as described in
41 (Martinez-Garcia and de Lorenzo, 2012) and selected in solid M9 minimal media supplemented
42 with 0.2% w/v citrate and appropriate antibiotics. Tetra-parental mating was used as described by
43 (Choi et al., 2005) to insert the mini-transposon Tn7-M-*P*_{EM7}-*gfp*-RBS⁻ into the *att*Tn7 site of *P.*
44 *putida* EM42, using M9-citrate-Gm as selective media (see below for details).

45

46 *Construction of plasmids and strains.*

47

48 The medium-high copy number plasmid pSEVA2514-*rec2*-*mutL*_{E36K}^{PP} (Supplementary Table S2)
49 was used for the construction of two derivatives bearing low- and medium- copy number origins
50 of replication. This plasmid was cut with PacI/SpeI and the 4.2 Kb DNA band, containing the *rec2*
51 and *mutL*_{E36K}^{PP} genes under the control of the thermo-inducible system *cl857/P_L*, was ligated to
52 PacI/SpeI restricted plasmids pSEVA221 (low copy number) and pSEVA231 (medium copy
53 number). Ligations were transformed into *E. coli* CC118 and selection was made in LB-Km
54 plates, obtaining plasmids pSEVA2214-*rec2*-*mutL*_{E36K}^{PP} and pSEVA2314-*rec2*-*mutL*_{E36K}^{PP}. Both
55 constructs were separately introduced in *P. putida* EM42 by tri-parental matings followed by
56 selection in M9-citrate-Km solid media, obtaining the strains *P. putida* EM42 (pSEVA2214-*rec2*-
57 *mutL*_{E36K}^{PP}) and *P. putida* EM42 (pSEVA2314-*rec2*-*mutL*_{E36K}^{PP}). *P. putida* EM42 was also
58 transformed by the same method with pSEVA2314, generating the control strain *P. putida* EM42
59 (pSEVA2314). A Tn7 mini-transposon with the *gfp* gene under the control of the constitutive *P*_{EM7}
60 promoter, but lacking the ribosome binding site (RBS) sequence, was constructed. To this end,
61 first the *gfp* gene was placed under the control of the *P*_{EM7} promoter: plasmid pSEVA637
62 (Supplementary Table S2) was cut with HindIII/SpeI and the purified 0.7 Kb band (RBS + *gfp*

63 gene) was ligated to the pSEVA237R-PEM7 (Supplementary Table S2) backbone digested with
64 HindIII/SpeI. Upon transformation in *E. coli* CC118 and selection on LB-Km plates, the resulting
65 plasmid (pSEVA237-PEM7) was digested with PacI/SpeI and the purified 0.9 Kb band (containing
66 the *gfp* gene under the control of the P_{EM7} and bearing a consensus 5'-AGGAGG-3' RBS
67 sequence) was ligated to a pTn7-M plasmid restricted with the same enzymes. Ligation mixture
68 was used to transform *E. coli* competent cells and selection was done in LB-KmGm plates. The
69 resulting plasmid, pTn7-M-PEM7-GFP, was used as a template to eliminate the RBS sequence.
70 In order to achieve this, the plasmid was PCR amplified with primers Tn7-PEM7-F/ Tn7-PEM7-R
71 ($T_m = 58$ °C, 2 min. elongation, Q5 polymerase). The primers were designed to i) amplify the
72 whole plasmid with the exception of the 7-nt Shine Dalgarno motif 5'-AGGAGGA-3' located 7-nt
73 away from the *gfp* start codon, ii) generate a PCR product sharing a 40-bp sequence at both
74 sides of the molecule to allow isothermal assembly of the amplicon. The 3.9 Kb PCR product was
75 purified and subjected to Gibson Assembly and the reaction was transformed into *E. coli*.
76 Selection was made in LB-KmGm plates, thus obtaining the plasmid pTn7-M-PEM7-GFP-RBS⁻.
77 The region between the P_{EM7} promoter and the end of the *gfp* gene was fully sequenced with
78 primers PS2 and PEM7-F to ensure the correct deletion of the RBS sequence. *E. coli* (pTn7-M-
79 PEM7-GFP-RBS⁻) was used as the donor strain to introduce the mini-transposon in the *attTn7*
80 site of *P. putida* EM42. Both strains and the helper strains *E. coli* HB101 (pRK600) and *E. coli*
81 (pTNS2) were used in a tetra-parental mating followed by selection in M9-citrate-Gm solid media.
82 Colonies were streaked in the same media and subjected to two diagnostic PCRs to check the
83 mini-transposon insertion. PCRs with primer pairs PS2/ PP5408-F ($T_m = 60$ °C, 1 min. 30
84 seconds elongation) and PEM7-F/Tn7-GlmS ($T_m = 60$ °C, 1 min. elongation) yielded bands of 2.2
85 Kb and 1.2 Kb, respectively, confirming the correct integration of the transposon in the *attTn7*
86 locus. The resulting strain *P. putida* EM42::Tn7-M- P_{EM7} -*gfp*-RBS⁻ (referred as *P. putida* TA245 in
87 Supplementary Table S2) was transformed by tripartite mating with pSEVA2314-*rec2*-*mutL*_{E36K}^{PP}
88 plasmid. After selection on M9-citrate-KmGm plates, the strain *P. putida* TA245 (pSEVA2314-
89 *rec2*-*mutL*_{E36K}^{PP}) was obtained. Integrity of the constructs described above, either in *E. coli* or *P.*
90 *putida*, was always checked by miniprep, restriction and agarose gel visualization.

91

92 *Oligonucleotide design, recombineering protocol, cycling procedure and screening*

93

94 The nine oligonucleotides used in this work for recombineering experiments (SR, NR, RR, PR,
95 CR, RBS-C₆, RBS-Deg₆, RBS-C₉, RBS-Deg₉) were designed to introduce different allelic changes
96 targeting the lagging strand of the *P. putida* chromosome. Supplementary Table S3 summarizes
97 the main features of each oligonucleotide while complete sequence and additional details can be
98 found in Supplementary Table S1. The recombineering protocol used here relies in the co-
99 expression of the Rec2 recombinase and the MutL_{E36K}^{PP} dominant negative allele from plasmids
100 endowed with the thermo-inducible cI857/P_L expression system (pSEVA2214-*rec2-mutL*_{E36K}^{PP},
101 pSEVA2314-*rec2-mutL*_{E36K}^{PP} or pSEVA2514-*rec2-mutL*_{E36K}^{PP}). The protocol is basically identical to
102 that described previously in (Aparicio et al., 2019b). Overnight cultures of *P. putida* strains
103 harboring the proper plasmid were used to inoculate 20 ml of fresh LB-Km at OD₆₀₀ = 0.1 in 100
104 ml Erlenmeyer flasks. Cultures were incubated at 30 °C with vigorous shaking (170 rpm) until
105 OD₆₀₀ ~ 1.0 and flasks were then placed in a water bath at 42 °C for 5 minutes to increase rapidly
106 the temperature and induce the P_L promoter. Ten additional minutes of incubation at 42 °C was
107 performed in an air shaker at 250 rpm (induction total time at 42 °C= 15 minutes) to trigger the
108 expression of *rec2-mutL*_{E36K}^{PP} genes, followed by 5 minutes in ice to cool down the bacterial
109 culture and stop the induction. Competent cells were then prepared transferring 10 ml of each
110 culture to 50-ml conical tubes and centrifuging the cells at 3,220 g/ 5 minutes. Cell pellets were
111 resuspended in 10 ml of 300 mM sucrose and washed two additional times with 5 and 1 ml of the
112 same solution. After centrifugation in a bench-top centrifuge (10,000 rpm, 1 minute), cellular
113 pellets were finally resuspended in 200 µl of 300 mM sucrose and 100 µl of this suspension was
114 added with the recombineering oligonucleotide. For single-oligonucleotide experiments, 1 µl from
115 a 100 µM stock was used (1 µM final concentration). For multiplexed experiments, 10 µl of each
116 oligonucleotide stock at 100 µM (SR, NR, RR, PR and CR) were mixed and 3 µl of this mixture
117 were added to the competent cells (accounting for 0.6 µM of each oligo.). The cell suspension
118 was mixed thoroughly by pipetting, placed in an electroporation cuvette (Bio-Rad, 2 mm-gap
119 width) and electroporated at 2.5 kV in a Micropulser™ device (Bio-Rad Laboratories, Hercules,
120 CA, USA). Cells were immediately inoculated in 5 ml of fresh TB in 100 ml Erlenmeyer flasks and
121 recovered at 30 °C/ 170 rpm. Before plating the cells for screening of allelic replacements,
122 different recovery times and TB additions were used depending on the experiment. For one cycle
123 recombineering experiments, overnight recovery was done in TB for assays with SR and NR
124 oligonucleotides while for experiments with oligonucleotides RBS-C₆, RBS-Deg₆, RBS-C₉ and RBS-

125 Degg, TB supplemented with Km and Gm was preferred. Specifications for cycled recombineering
126 assays (HEMSE) are depicted below.

127

128 *High-efficiency multi-site genomic editing protocol*

129

130 HEMSE is a cycled recombineering protocol run in a multiplexed fashion. The procedure involves
131 a standard recombineering protocol in which, as explained before, cultures were subjected to
132 electrotransformation with an equimolar mixture of several oligonucleotides. The recovery was
133 performed in TB added with Km in order to maintain the plasmid along the cycles, and the
134 incubation proceeded at 30 °C with vigorous shaking (170 rpm) until an $OD_{600} \sim 1.0$ (Cycle-I).
135 Culture aliquots were withdrawn for screening and the bacterial culture entered in the next round
136 of recombineering by performing induction at 42 °C/ 15 minutes, competent cell preparation,
137 oligonucleotide mixture electroporation and recovery till reaching again a cell density around 1.0
138 at 600 nm (Cycle-II). Further cycles proceeded in the same way (Fig. 3 of main text). Each cycle
139 took one day in average and recovery, when necessary, was performed overnight at room
140 temperature without shaking to avoid culture overgrowth. When recovery step was completed at
141 the end of the day, cultures were stored at 4 °C overnight. A new cycle was started in the next
142 morning incubating the culture 30 minutes at 30 °C (170 rpm) before the induction step.
143 Screening of allelic changes after recombineering was performed plating aliquots of recovered
144 cultures in the appropriate selective and/or non-selective solid media, as follows:

145

146 • In single-oligonucleotide experiments with SR and NR oligonucleotides (one cycle), overnight
147 cultures were plated in LB-Sm (dilutions 10^{-4} and 10^{-5}) and LB-Nal (dilutions 10^{-4} and 10^{-5}),
148 respectively, to estimate the allelic replacements, while dilutions 10^{-7} and 10^{-8} were done in LB
149 without antibiotics to count viable cells. Plates were incubated 18 h. at 30 °C and CFUs
150 annotated.

151

152 • In single-oligonucleotide experiments with RBS-C₆, RBS-Deg₆, RBS-C₉, RBS-Deg₉ oligos (one
153 cycle), cultures recovered overnight were plated on 150 mm width LB-KmGm-activated charcoal
154 plates using 10^{-6} dilutions. This allowed an average of 500 colonies per plate. To facilitate the
155 identification of colonies displaying low levels of fluorescence, plates were incubated at 30 °C for

156 5 days. Fluorescent colonies were streaked in the same media and insertion of putative ribosome
157 binding sites upstream the *gfp* gene were checked by PCR amplifying this DNA region with
158 primers PS2/ PP5408-F ($T_m = 60\text{ }^\circ\text{C}$, 1 min. 30 seconds elongation, 1.0 Kb product) and
159 sequencing the amplicon with primer ME-I-Gm-ExtR. Non-redundant clones with different
160 sequences inserted were selected and glycerol stocks made prior characterization by flow
161 cytometry.

162

163 • Allelic replacements in HEMSE experiments were screened after recovery steps ($OD_{600} \sim 1.0$)
164 of cycle-I, cycle-V and cycle-X. Viable cells were estimated plating dilutions 10^{-7} and 10^{-8} in LB
165 plates. Single mutants coming from SR-, NR-, RR- and PR-mediated recombineering were
166 analyzed by plating dilutions 10^{-4} and 10^{-5} in LB-Sm, LB-Nal, LB-Rif and LB-5FOA-Ura plates.
167 Plates were incubated 24 h at $30\text{ }^\circ\text{C}$ and total CFUs of single mutants (Sm^R , Nal^R , Rif^R and
168 $5FOA^R$) and viable cells were taken. Twenty $5FOA^R$ colonies were replicated on M9-citrate and
169 M9-citrate-5FOA-Ura plates in order to discriminate authentic *pyrF* mutants ($5FOA^R/Ura^-$) from
170 spontaneous $5FOA^R$ mutants ($5FOA^R/Ura^+$), as stated in (Galvao and de Lorenzo, 2005; Aparicio
171 et al., 2016). Colonies grown on both media were discounted of the total $5FOA^R$ numbers as
172 *pyrF*-unrelated, spontaneous mutants. Dilutions 10^{-6} in LB-benzoate plates allowed the estimation
173 of *catA-I*⁻ mutants simply by counting the dark-brown colonies appeared after 10 days of
174 incubation at $30\text{ }^\circ\text{C}$. *catA-I*⁻ mutants accumulate catechol, which turns into brown intermediates
175 after spontaneous oxidation and polymerization (Jimenez et al., 2014). In previous assays aimed
176 to obtain *catA-I*⁻ mutants through recombineering with CR oligo, it was noticed that long
177 incubations were necessary to appreciate the colored phenotype in solid media (Fig. S2). The
178 observed dark-brown colonies were always *catA-I*⁻ mutants, as was demonstrated by
179 amplification of *catA-I* gene (primers *catA-F/catA-R*, $T_m = 55\text{ }^\circ\text{C}$, 1 minute elongation) and
180 sequencing of the 0.5 Kb amplicon with primer *catA-F* (data not shown) in 20 selected colonies.
181 Multiple gene editions were also analyzed plating cultures from cycles I, V and X on LB solid
182 media supplemented either with Sm+Nal+ Rif+5FOA+Ura (four editions mediated by SR, NR, RR
183 and PR oligonucleotides), 24 incubation at $30\text{ }^\circ\text{C}$, or with Sm+Nal+Rif+5FOA+Ura+benzoate (five
184 editions mediated by the 5 oligonucleotides used in this study), 10 days incubation at $30\text{ }^\circ\text{C}$. For
185 this last experiment, there were considered quintuple mutants those colonies displaying
186 resistance to Sm, Nal, Rif and 5FOA and also showing the characteristic brown phenotype of

187 *catA*⁻ mutants. The recombineering frequency (RF) was calculated as the ratio between the
188 number of colonies showing a given phenotype and the number of viable cells within the
189 experiment, being this ratio normalized to 10⁹ viable cells for graphic representation.

190

191 In order to check the accuracy of the allelic replacements, 18 colonies showing the quintuple
192 mutant phenotype (Sm^R, Nal^R, Rif^R, 5FOA^R and catechol accumulation) were checked by PCR
193 amplification and sequencing of the target genes. For each bacterial clone, five different PCRs
194 were set up to amplify: *rpsL* (primers *rpsL*-Fw/ *rpsL*-Rv, T_m 57 °C, 45 seconds elongation, 0.8 Kb
195 product), *gyrA* (primers *gyrA*-Fw/ *gyrA*-Rv, T_m 57 °C, 45 seconds elongation, 0.4 Kb product),
196 *rpoB* (primers *rpoB*-F/*rpoB*-R, T_m 57 °C, 45 seconds elongation, 0.4 Kb product), *pyrF* (primers
197 *pyrF*-F/*pyrF*-R, T_m 52 °C, 1 minute elongation, 1.2 Kb product) and *catA-I* (primers *catA*-F/*catA*-
198 R, T_m 55 °C, 1 minute elongation, 0.5 Kb product). The purified PCR products were sequenced
199 with the putative forward primers and the sequence analysed for the expected changes mediated
200 by recombineering. All clones analysed (n=18; 100%) showed the correct changes,
201 demonstrating that the observed phenotypes corresponded to mutations mediated by the HEMSE
202 procedure. Single allelic replacements in HEMSE experiments were not confirmed by PCR and
203 sequencing since previous works showed that virtually 100 % of Sm^R, Nal^R and *pyrF*⁻ mutants
204 obtained by recombineering with oligos SR, NR and LM (almost identical to RR oligo used in this
205 work) harbored the expected changes in the target genes *rpsL*, *gyrA* and *pyrF* (Ricaurte et al.,
206 2018) (Aparicio et al., 2019a). Preliminary studies in this work showed, on the other hand, that
207 single Rif^R mutants also displayed 100 % accuracy in the expected mutations of the target gene
208 *rpoB* (data not shown). As explained before, *catA*⁻, dark-brown colonies were also analyzed by
209 PCR and sequencing in previous test experiments (data not shown), with analogous results.

210

211 *Flow cytometry*

212

213 The visual selection of fluorescent colonies from recombineering experiments with oligos RBS-
214 Deg₆ and RBS-Deg₉ gave rise to a collection of 31 RBS insertion mutants showing a wide variety
215 of fluorescent signals. Together with the negative controls of *P. putida* TA245 (insertion of Tn7-M-
216 P_{EM7}-*gfp*-RBS⁻) and *P. putida* EM42 (no *gfp* gene), a total of 33 strains were characterized for
217 GFP production. Each strain was inoculated from glycerol stocks in 2 ml of LB-KmGm (*P. putida*

218 EM42 in LB; *P. putida* TA245 in LB-Gm) and cultured at 30 °C/ 170 rpm. 0.5 ml of overnight
219 cultures ($OD_{600} \sim 2-3$) were centrifuged and resuspended in 1 ml of filtered Phosphate Buffered
220 Saline (PBS) 1X (8mM Na₂HPO₄, 1.5mM KH₂PO₄, 3mM KCl, 137mM NaCl, pH.7.0). Fifty μ l of
221 each suspension was added to 450 μ l of PBS 1X to obtain cellular samples with $OD_{600} \sim 0.1-$
222 0.15 . Samples were analyzed in a MACSQuantTM VYB cytometer (Miltenyi Biotec, Bergisch
223 Gladbach, Germany) to quantify the emission of fluorescence as indicated in (Martinez-Garcia et
224 al., 2014). GFP was excited at 488 nm and the fluorescence signal was recovered with a 525 ± 40
225 nm band-pass filter. For each sample, at least 100,000 events were analyzed and the FlowJo v.
226 9.6.2 software (FlowJo LLC, Ashland, OR, USA) was used to process the results. Population was
227 gated to eliminate background noise and the median of the GFP-A channel of two biological
228 replicas was used for graphical representation.

229

230

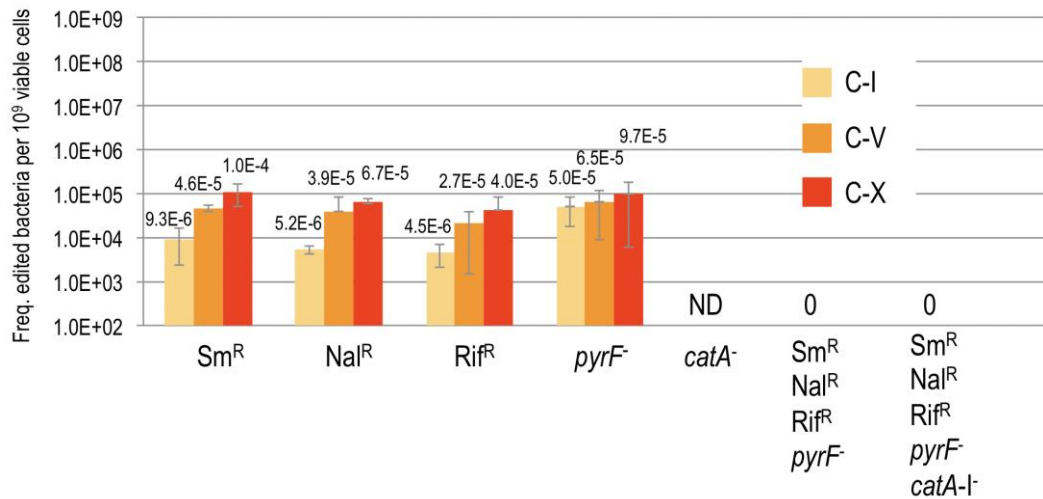
231

SUPPLEMENTARY FIGURES

232

233

Figure S1. Rec2-independent editing in HEMSE assays



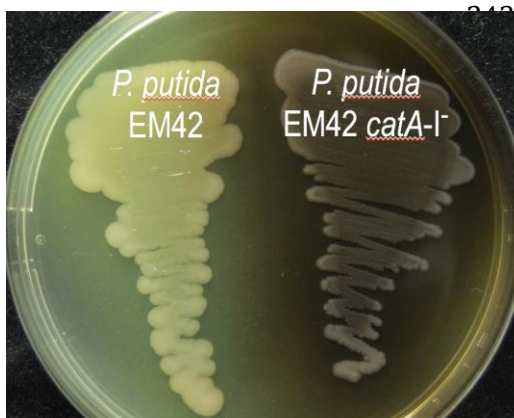
234

235 Editing efficiencies of single and multiple changes in the control strain *P. putida* EM42 harboring
236 the empty plasmid pSEVA2314 were assayed applying 10 cycles of HEMSE and an equimolar
237 mixture of oligos SR, NR, RR, PR and CR, following the same procedure explained in Figure 4A
238 and 4B. See more details in Transparent Methods section. Allelic replacements of *catA-I* gene
239 were not determined in these assays (ND), while multiple editions could not be detected (0).

240

241 **Figure S2.** Phenotype of *P. putida* EM42 *catA-I*⁻ strain

242



P. putida EM42 (pSEVA2314-*rec2-mut*_{L_{E36K}}^{PP}) was subjected to recombineering with CR oligonucleotide (see Transparent Methods section). Three stop codons were inserted in the *catA-I* ORF, generating a mutant strain in which the metabolism of benzoic acid is impaired, leading to accumulation of catechol (Jimenez et al., 2014). Upon spontaneous

251 oxidation and polymerization, catechol derivatives exhibit a characteristic dark-brown colour. *P.*
252 *putida* EM42 and the *catA-I*⁻ mutant were grown in LB-Agar supplemented with benzoate 5 mM
253 and incubated 10 days at 30 °C to allow the visualization of the colored phenotype.

254

255

SUPPLEMENTARY TABLES

256

257 **SUPPLEMENTARY TABLE S1.** Oligonucleotides used in this study.

258

Name	^(a) Sequence (5' → 3')	Usage / Source
SR	G*T*C*A*GACGCACACGGCATACTTTACGCAG TGCCGAGTTAGTTTTGTCGGCGTGGTGGTG TACACACGGGTGCACACGCCACGACGCTGC	Recombineering oligo for <i>rpsL</i> gene: AAA (K43) changed to ACA (T43), mismatch A:G, confers Sm resistance (Ricaurte et al., 2018)
rpsL-Fw	GACATGAAATGTTGCCGATG	To amplify and sequence part of <i>rpsL</i> gene of <i>P. putida</i> (Ricaurte et al., 2018)
rpsL-Rv	CTGTTCTTGCGTGCTTTGAC	With rpsL-Fw, to amplify part of <i>rpsL</i> gene of <i>P. putida</i> (Ricaurte et al., 2018)
NR	AACGAGAACGGCTGGGCCATACGCACGATGG TATTGTAGACCGCAGTGTCCCGTGCGGGTG GTA	Recombineering oligo for <i>gyrA</i> gene: GAC (D87) changed to AAT (N87), mismatches G:T and C:A, confers Nal resistance (Aparicio et al., 2019b)
gyrA-F	GGCCAAAGAAATCCTCCCGGTCAA	To amplify and sequence part of <i>gyrA</i> gene of <i>P. putida</i> (Aparicio et al., 2019b)
gyrA-R	AGCAGGTTGGGAATACGCGTCCG	To amplify and sequence part of <i>gyrA</i> gene of <i>P. putida</i> (Aparicio et al., 2019b)
RR	TCCGAGAGAGGGTTGTTCTGGTCCATGAACA GGGACAGCTGGCTGGAACCGAAGAACTCT	Recombineering oligo for <i>rpoB</i> gene: CAG (Q518) changed to CTG (L518), mismatch A:A, confers Rif resistance. This work
rpoB-F	CCTGGGTAACCGTCGCGTACGGTG	To amplify and sequence part of <i>rpoB</i> gene of <i>P. putida</i> . This work
rpoB-R	CGCCTTCCTTACCACGCGGTACG	To amplify and sequence part of <i>rpoB</i> gene of <i>P. putida</i> . This work
PR	AGGTCCAGGAACACTTCAAGCCCTTGTCACA CAGGGTTTAGACAATGCCCGAAGCGCTGCTG GTGAACAGCTCCTTGCCA	Recombineering oligo for <i>pyrF</i> gene: GAA (E50) changed to TAA (Stop), mismatch A:G, confers 5FOA resistance and uracil

		auxotrophy. This work
pyrF-F	CGAGGGCTATGATGAGTATC	To amplify and sequence the <i>pyrF</i> gene of <i>P. putida</i> (Aparicio et al., 2016)
pyrF-R	GTCAGGTGAAGAGCAAAGAG	To amplify and sequence the <i>pyrF</i> gene of <i>P. putida</i> (Aparicio et al., 2016)
CR	GCAGCACGCGCAGAATGATCTGCTTGAAGCG CGGGTTTCCCTATTATCAATTCGGCATGGTCCA GGCCAGCTACCCGGTTGAAGAAGGCT	Recombineering oligo for <i>catA-I</i> gene: insertion of three stop codons truncates the ORF, giving rise to brown colonies in presence of benzoate. This work
catA-F	AACTCGTCCTCGGTAATCTC	To amplify and sequence part of <i>catA-I</i> gene of <i>P. putida</i> . This work
catA-R	CAGCAATCAAGGAGATAACC	To amplify and sequence part of <i>catA-I</i> gene of <i>P. putida</i> . This work
Tn7-PEM7-F	AAAACATATGAGTAAAGGAGAAGAAGCTTTTCA	To remove RBS sequence from pTn7-M-PEM7-GFP by Gibson Assembly. This work
Tn7-PEM7-R	AACTCCAGTGAAAAGTTCTTCTCCTTTACTCAT ATGTTTTAAGCTTGCATGCCTGCAGGTCG	To remove RBS sequence from pTn7-M-PEM7-GFP by Gibson Assembly. This work
PEM7-F	AATACGACAAGGTGAGGAAC	To amplify and sequence from P_{EM7} promoter. This work
PP5408-F	CGATTCATCAGGTTGGATTCG	To amplify and sequence mini-Tn7 insertions from PP_5408 locus of <i>P. putida</i> . This work
Tn7-GlmS	AATCTGGCCAAGTCGGTGAC	To amplify and sequence mini-Tn7 insertions from <i>glmS</i> gene of <i>P. putida</i> (Lambertsen et al., 2004)
PS2	GCGGCAACCGAGCGTTC	To amplify and sequence from T_0 terminator (Silva-Rocha et al., 2013)
ME-I-Gm-ExtR	GTTCTGGACCAGTTGCGTGAG	To amplify and sequence from mini-Tn7 Gm resistance gene (Martinez-Garcia et al., 2014)

RBS-C ₆	TCTAGAGTCGACCTGCAGGCATGCAAGCTTA GGAGG AAAAACATATGAGTAAAGGAGAAGAA CTTTT	Recombineering oligo to insert a consensus 6 nucleotide RBS sequence upstream the <i>gfp</i> gene in strains Tn7-M-P _{EM7-gfp} -RBS ⁻ . This work
RBS-Deg ₆	TCTAGAGTCGACCTGCAGGCATGCAAGCTTR RRRRR AAAAACATATGAGTAAAGGAGAAGAAC TTTT	Recombineering oligo to insert a degenerated (R=A,G) 6 nucleotide RBS sequence upstream the <i>gfp</i> gene in strains Tn7-M-P _{EM7-gfp} -RBS ⁻ . This work
RBS-C ₉	TCTAGAGTCGACCTGCAGGCATGCAAGCTTTA AGGAGGT AAAAACATATGAGTAAAGGAGAAGA ACTTTT	Recombineering oligo to insert a consensus 9 nucleotide RBS sequence upstream the <i>gfp</i> gene in strains Tn7-M-P _{EM7-gfp} -RBS ⁻ . This work
RBS-Deg ₉	TCTAGAGTCGACCTGCAGGCATGCAAGCTTTA RRRRRRR TAAAAACATATGAGTAAAGGAGAAGA ACTTTT	Recombineering oligo to insert a degenerated (R=A,G) 9 nucleotide RBS sequence upstream the <i>gfp</i> gene in strains Tn7-M-P _{EM7-gfp} -RBS ⁻ . This work

259

260 ^(a) Asterisks denote phosphorothioate bonds. Single changes introduced by recombineering
 261 oligonucleotides SR, NR, RR and PR are highlighted in bold. The three stop codons inserted by oligo CR
 262 appear in blue. The sequences encompassing the stretch inserted by the four RBS-X oligos are shown in
 263 red color.

264

265

266 **SUPPLEMENTARY TABLE S2.** Bacterial strains and plasmids used in this work.

267

Strain or plasmid	Relevant characteristics ^a	Reference or source
<i>Escherichia coli</i>		
CC118	Cloning host; $\Delta(\text{ara-leu}) \text{ araD } \Delta\text{lacX174 galE galK phoA thiE1 rpsE}(\text{Sp}^{\text{R}}) \text{ rpoB}(\text{Rif}^{\text{R}}) \text{ argE}(\text{Am}) \text{ recA1}$	(Manoil and Beckwith, 1985)
HB101	Helper strain used for conjugation; $\text{F}^{-} \lambda^{-} \text{ hsdS20}(\text{rB}^{-} \text{ mB}^{-}) \text{ recA13 leuB6}(\text{Am}) \text{ araC14 } \Delta(\text{gpt-proA})62 \text{ lacY1 galK2}(\text{Oc}) \text{ xyl-5 mtl-1 thiE1 rpsL20}(\text{Sm}^{\text{R}}) \text{ glnX44 (AS)}$	(Boyer and Roulland-Dussoix, 1969)
CC118 λ pir	Cloning host for plasmids containing an R6K origin of replication; $\Delta(\text{ara-leu}) \text{ araD } \Delta\text{lac X174 galE galK phoA20 thi-1 rpsE rpoB argE (Am) recA1, } \lambda\text{pir lysogen}$	(Herrero et al., 1990)
<i>Pseudomonas putida</i>		
EM42	KT2440 derivative; $\Delta\text{prophage1 } \Delta\text{prophage4 } \Delta\text{prophage3 } \Delta\text{prophage2 } \Delta\text{Tn7 } \Delta\text{endA-1 } \Delta\text{endA-2 } \Delta\text{hsdRMS } \Delta\text{flagellum } \Delta\text{Tn4652}$	(Martinez-Garcia et al., 2014)
TA238	EM42 derivative; $\text{rpsL}^{-}(\text{Sm}^{\text{R}}) \text{ gyrA}^{-}(\text{Nal}^{\text{R}}) \text{ rpoB}^{-}(\text{Rif}^{\text{R}}) \text{ pyrF}^{-}(\text{5FOA}^{\text{R}}) \text{ catA-I}^{-}$	This work
TA245	EM42 derivative with mini-Tn7-M-P _{EM7} -gfp-RBS ⁻ transposon inserted in the attTn7 site	This work
Plasmids		
pSEVA2314	Inducible expression vector; <i>oriV</i> (pBBR1); cargo [cl857-P _L]; standard multiple cloning site; Km ^R	(Aparicio et al., 2019a)
pSEVA2214- <i>rec2</i> - <i>mutL</i> _{E36K} ^{PP}	pSEVA2214 derivative bearing the <i>rec2</i> recombinase and <i>mutL</i> _{E36K} ^{PP} allele ; <i>oriV</i> (RK2); cargo [cl857-P _L → <i>rec2</i> - <i>mutL</i> _{E36K} ^{PP}]; Km ^R	This work GenBank n° MN688223
pSEVA2314- <i>rec2</i> - <i>mutL</i> _{E36K} ^{PP}	pSEVA2314 derivative bearing the <i>rec2</i> recombinase and	This work

	<i>mutL_{E36K}^{PP}</i> allele ; <i>oriV</i> (pBBR1); cargo [<i>cl857-P_L</i> → <i>rec2-</i>	GenBank n°
	<i>mutL_{E36K}^{PP}</i>]; Km ^R	MN688222
pSEVA2514- <i>rec2- mutL_{E36K}^{PP}</i>	pSEVA2514 derivative bearing the <i>rec2</i> recombinase and	(Aparicio et al.,
	<i>mutL_{E36K}^{PP}</i> allele ; <i>oriV</i> (RFS1010); cargo [<i>cl857-P_L</i> →	2019b)
	<i>rec2-mutL_{E36K}^{PP}</i>]; Km ^R	GenBank n°
		MN180222
pSEVA637	<i>oriV</i> (pBBR1); cargo [<i>gfp</i>]; Gm ^R	(Silva-Rocha et
		al., 2013)
		(Martinez-
		Garcia et al.,
		2015)
pSEVA237R-PEM7	<i>oriV</i> (pBBR1); cargo [<i>P_{EM7}</i> → <i>mCherry</i>]; Km ^R	(Silva-Rocha et
		al., 2013)
		(Martinez-
		Garcia et al.,
		2015)
pSEVA237-PEM7	<i>oriV</i> (pBBR1); cargo [<i>P_{EM7}</i> → <i>gfp</i>]; Km ^R	This work
pTn7-M	<i>oriV</i> (R6K); mini-Tn7 transposon; standard multiple cloning	(Zobel et al.,
	site; Km ^R Gm ^R	2015)
pTn7-M-PEM7-GFP	pTn7-M derivative with <i>P_{EM7}-gfp</i> in the mini-Tn7	This work
	transposon; Km ^R Gm ^R	
pTn7-M-PEM7-GFP-RBS ⁻	pTn7-M-PEM7-GFP derivative lacking the <i>gfp</i> RBS; Km ^R	This work
	Gm ^R	
pRK600	Helper plasmid used for conjugation; <i>oriV</i> (ColE1), RK2	(Kessler et al.,
	(<i>mob+</i> <i>tra+</i>); Cm ^R	1992)
pTNS2	Helper plasmid for mini-Tn7 transposition; <i>oriV</i> (R6K),	(Choi et al.,
	TnsABC+D specific transposition pathway; Ap ^R	2005)

268

269 ^a Antibiotic markers: Ap, ampicillin; Cm, chloramphenicol; Km, kanamycin; 5FOA, 5-fluoro-orotic acid;

270 Gm, gentamicin; Nal, nalidixic acid; Rif, rifampicin; Sm, streptomycin; Sp, spectinomycin.

271

272 **SUPPLEMENTARY TABLE S3.** Main features of recombineering oligonucleotides used in this study.

273

<u>Name</u>	<u>P-thioate bonds</u>	<u>Length</u>	<u>Target gene</u>	<u>Change/mismatch</u>	<u>MMR sensitivity</u>	<u>ΔG (kcal/mol)</u>	<u>Phenotype</u>
SR	Four at 5'-end	94	<i>rpsL</i>	A→C/A:G	Low	- 20.79	Sm ^R
NR	None	65	<i>gyrA</i>	G→A/ G:T C→T/ C:A	High	- 11.84	Nal ^R
RR	None	60	<i>rpoB</i>	A→T/ A:A	High	- 7.26	Rif ^R
PR	None	81	<i>pyrF</i>	G→T/ G:A	Low	- 14.03	5-FOA ^R /Ura ⁻
CR	None	89	<i>catA-I</i>	Insertion 3 Stops	Low	- 12.84	Catechol accumulation (Brown color)
RBS-C ₆	None	67	<i>gfp</i> UTR	Insertion 7 nt	Low	- 4.94	Fluorescent
RBS-Deg ₆	None	67	<i>gfp</i> UTR	Insertion 7 nt (deg.)	Low	Variable	Fluorescent
RBS-C ₉	None	70	<i>gfp</i> UTR	Insertion 10 nt	Low	- 4.59	Fluorescent
RBS-Deg ₉	None	70	<i>gfp</i> UTR	Insertion 10 nt (deg.)	Low	Variable	Fluorescent

274

275

276 REFERENCES

277

278 Aparicio, T., de Lorenzo, V., and Martinez-Garcia, E. (2019a) Improved thermotolerance of
279 genome-reduced *Pseudomonas putida* EM42 enables effective functioning of the P_L /cl857
280 System. *Biotechnol J* **14**: e1800483.

281 Aparicio, T., Jensen, S.I., Nielsen, A.T., de Lorenzo, V., and Martinez-Garcia, E. (2016) The Ssr
282 protein (T1E_1405) from *Pseudomonas putida* DOT-T1E enables oligonucleotide-based
283 recombineering in platform strain *P. putida* EM42. *Biotechnol J* **11**: 1309-1319.

284 Aparicio, T., Nyerges, A., Nagy, I., Pal, C., Martinez-Garcia, E., and de Lorenzo, V. (2019b)
285 Mismatch repair hierarchy of *Pseudomonas putida* revealed by mutagenic ssDNA
286 recombineering of the *pyrF* gene. *Environ Microbiol* doi: 10.1111/1462-2920.14814.

287 Boyer, H.W., and Roulland-Dussoix, D. (1969) A complementation analysis of the restriction and
288 modification of DNA in *Escherichia coli*. *J Mol Biol* **41**: 459-472.

289 Choi, K.H., Gaynor, J.B., White, K.G., Lopez, C., Bosio, C.M., Karkhoff-Schweizer, R.R., and
290 Schweizer, H.P. (2005) A Tn7-based broad-range bacterial cloning and expression
291 system. *Nat Methods* **2**: 443-448.

- 292 Galvao, T.C., and de Lorenzo, V. (2005) Adaptation of the yeast URA3 selection system to Gram-
293 negative bacteria and generation of a $\Delta betCDE$ *Pseudomonas putida* strain. *Appl Environ*
294 *Microbiol* **71**: 883-892.
- 295 Herrero, M., de Lorenzo, V., and Timmis, K.N. (1990) Transposon vectors containing non-
296 antibiotic resistance selection markers for cloning and stable chromosomal insertion of
297 foreign genes in gram-negative bacteria. *J Bacteriol* **172**: 6557-6567.
- 298 Jimenez, J.I., Perez-Pantoja, D., Chavarria, M., Diaz, E., and de Lorenzo, V. (2014) A second
299 chromosomal copy of the *catA* gene endows *Pseudomonas putida* mt-2 with an enzymatic
300 safety valve for excess of catechol. *Environ Microbiol* **16**: 1767-1778.
- 301 Kessler, B., de Lorenzo, V., and Timmis, K.N. (1992) A general system to integrate *lacZ* fusions
302 into the chromosomes of gram-negative eubacteria: regulation of the *Pm* promoter of the
303 TOL plasmid studied with all controlling elements in monocopy. *Mol Gen Genet* **233**: 293-
304 301.
- 305 Lambertsen, L., Sternberg, C., and Molin, S. (2004) Mini-Tn7 transposons for site-specific tagging
306 of bacteria with fluorescent proteins. *Environ Microbiol* **6**: 726-32.
- 307 Manoil, C., and Beckwith, J. (1985) *TnphoA*: a transposon probe for protein export signals. *Proc*
308 *Natl Acad Sci USA* **82**: 8129-8133.
- 309 Martinez-Garcia, E., and de Lorenzo, V. (2012) Transposon-based and plasmid-based genetic
310 tools for editing genomes of gram-negative bacteria. *Methods Mol Biol* **813**: 267-283.
- 311 Martinez-Garcia, E., Aparicio, T., de Lorenzo, V., and Nikel, P.I. (2014) New transposon tools
312 tailored for metabolic engineering of Gram-negative microbial cell factories. *Front Bioeng*
313 *Biotechnol* **2**: 46.
- 314 Martinez-Garcia, E., Aparicio, T., Goni-Moreno, A., Fraile, S., and de Lorenzo, V. (2015) SEVA
315 2.0: an update of the Standard European Vector Architecture for de-/re-construction of
316 bacterial functionalities. *Nucleic Acids Res* **43**: D1183-1189.
- 317 Ricaurte, D.E., Martinez-Garcia, E., Nyerges, A., Pal, C., de Lorenzo, V., and Aparicio, T. (2018)
318 A standardized workflow for surveying recombinases expands bacterial genome-editing
319 capabilities. *Microb Biotechnol* **11**: 176-188.
- 320 Sambrook, J., Fritsch, E.F., and Maniatis, T. (1989) *Molecular cloning: a laboratory manual*. Cold
321 Spring Harbor, NY: Cold Spring Harbor Laboratory Press.

- 322 Silva-Rocha, R., Martinez-Garcia, E., Calles, B., Chavarria, M., Arce-Rodriguez, A., de Las
323 Heras, A. et al. (2013) The Standard European Vector Architecture (SEVA): a coherent
324 platform for the analysis and deployment of complex prokaryotic phenotypes. *Nucleic
325 Acids Res* **41**: D666-675.
- 326 Zobel, S., Benedetti, I., Eisenbach, L., de Lorenzo, V., Wierckx, N., and Blank, L.M. (2015) Tn7-
327 based device for calibrated heterologous gene expression in *Pseudomonas putida*. *ACS
328 Synth Biol* **4**: 1341-1351.
- 329